Journal of
PERIODONTAL RESEARCH

J Periodont Res 2010; 45: 626–634

JOURNAL OF PERIODONTAL RESEARCH
doi:10.1111/j.1600-0765.2010.01277.x

Butyrate, a bacterial metabolite, induces apoptosis and autophagic cell death in gingival epithelial cells

H. Tsuda[1,2], K. Ochiai[3,4], N. Suzuki[1,2], K. Otsuka[1,2]

[1]Department of Biochemistry, Nihon University School of Dentistry, Tokyo, Japan, [2]Divisions of Functional Morphology, Dental Research Center, Nihon University School of Dentistry, Tokyo, Japan, [3]Department of Oral Microbiology, Nihon University School of Dentistry, Tokyo, Japan and [4]Divisions of Immunology and Pathobiology, Dental Research Center, Nihon University School of Dentistry, Kanda Surugadai Chiyoda-ku, Tokyo, Japan

Tsuda H, Ochiai K, Suzuki N, Otsuka K. Butyrate, a bacterial metabolite, induces apoptosis and autophagic cell death in gingival epithelial cells. J Periodont Res 2010; 45: 626–634. © 2010 John Wiley & Sons A/S

Background and Objective: Butyrate is produced by some types of anaerobic periodontal bacteria. Millimolar concentrations of butyrate are found in mature dental plaque from periodontitis patients. Although butyrate reportedly has a variety of effects in many mammalian cells, its effect on gingival epithelial cells is not well known. In this study, we investigated the effect of butyrate on gingival epithelial Ca9-22 cell death.

Material and Methods: Death of Ca9-22 cells was assessed after treating the cells with or without butyrate. A SYTOX Green dye, which exhibits strong green fluorescence once it enters dead cells through ruptured cell membranes, was used for cell death detection. Phosphatidylserine redistribution was measured using fluorescein isothiocyanate-labeled annexin V. The activity of caspase-3 was measured as the amount of cleaved substrate peptide. Anti-apoptotic *bcl-2* mRNA expression was measured using real-time RT-PCR. Western blotting and fluoromicroscopic analysis with anti-microtubule-associated protein 1 light chain 3 (LC3) antibodies were performed for detection of autophagy.

Results: Stimulation with millimolar concentrations of butyrate for 48 h induced Ca9-22 cell death. The stimulation also caused increased caspase-3 activity, phosphatidylserine redistribution and *bcl-2* down-regulation, suggesting butyrate-induced apoptosis. However, the pan-caspase inhibitor, Z-VAD-FMK, did not inhibit cell death completely. This implies the existence of other types of cell death. In addition, markers of autophagy, namely, the conversion of LC3-I to LC3-II and increased LC3 accumulation, were observed. Moreover, inhibition of autophagy by 3-methyladenine suppressed the butyrate-induced cell death, suggesting that butyrate could induce cell death through autophagy.

Conclusion: These data suggest that butyrate induces apoptosis and autophagic cell death.

Hiromasa Tsuda, DDS, PhD, Department of Biochemistry, Nihon University School of Dentistry, 1-8-13 Kanda-Surugadai, Chiyoda-ku, 101-8310 Tokyo, Japan
Tel: +81 3 3219 8123
Fax: +81 3 3219 8334
e-mail: tsuda-h@dent.nihon-u.ac.jp

Key words: butyrate; autophagic cell death; apoptosis; gingival epithelial cell

Accepted for publication January 13, 2010

Periodontal diseases, which are common infectious diseases characterized by the inflammation and destruction of periodontal tissue including the alveolar bone, are caused by anaerobic gram-negative periodontopathic bacteria, such as *Porphyromonas*, *Prevotella* and *Fusobacterium* species. These bacteria colonize and accumulate in

gingival crevices as dental plaque and produce a variety of virulence factors, such as lipopolysaccharides, proteases, fimbriae, and capsular polysaccharides. These bacterial components reportedly induce effectors of inflammation in the gingival crevices and trigger periodontal tissue destruction. Periodontopathic bacteria also produce a high amount of butyrate, which is reported to have the following physiological functions: inhibition of gingival fibroblast proliferation (1,2), colon cancer cell growth (3) and phagocytosis by lung phagocytes (4); and stimulation of T-cell apoptosis (5), osteoblast maturation (6,7) and proinflammatory cytokine release by neutrophils (8). Since millimolar concentrations of butyrate are found in mature dental plaque (9), butyrate is thought to play an important role in the development of periodontitis (2,10–14).

There are two types of programmed cell death, apoptosis and autophagic cell death (15). Apoptosis is characterized by a series of biochemical events that lead to a variety of morphological changes, such as the loss of cell membrane asymmetry accompanied by phosphatidylserine translocation from the inner cell membrane to the cell surface, cell shrinkage, nuclear fragmentation, chromatin condensation and chromosomal DNA fragmentation (16–18). These phenomena are primarily regulated by two different signaling pathways, a mitochondrial pathway and a mitochondria-independent pathway. In the former, intramitochondrial apoptotic effectors leak into the cytoplasm and are assembled into apoptosomes; this results in the activation of caspase-3, a serine protease that produces several important morphological changes in apoptotic cells. Anti-apoptotic Bcl-2 family proteins, Bcl-2 and Bcl-XL, inhibit the leakage of intramitochondrial apoptotic effectors and prevent apoptosis. The activation of death receptors also induces apoptosis through the other apoptosis signaling cascade.

Autophagy is the process of recycling cytoplasmic materials during nutrient shortages. In this process, cytoplasmic components are engulfed by double-membraned structures (autophagosomes) and delivered to lysosomes for degradation (autophagolysosomes). The degraded components are then recycled to generate energy or for organelle synthesis. Furthermore, the activation of autophagy is an effective method of eliminating damaged organelles and infectious organisms within the cytosol (19). These roles of autophagy are important for cell survival. Paradoxically, autophagy has also been reported to be involved in a type of programmed cell death (20,21). Some morphological features that are characteristic of autophagy have been observed in a variety of cell types during development and tissue homeostasis, and on exposure to toxic chemicals (15). However, the exact role of autophagy is still unknown. Recently, some studies have reported that complex interrelationships exist between apoptosis and autophagy (20–24). For example, it has been reported that stimulants of apoptosis can induce cell death in conditions of impaired apoptotic signaling and this phenomenon is inhibited by blocking autophagic signaling (25), and that several pro-apoptotic signals induce autophagy (21). The complex relationship between mechanisms of apoptosis and autophagy is now the subject of considerable research.

The epithelial cells that line the gingival epithelial crevice form an important barrier, which physically protects highly vascularized subgingival connective tissues from bacterial invasion. In addition, the cells are also able to sense and respond to bacteria and their products. Therefore, gingival epithelial cells may be strongly influenced by butyrate, a major byproduct of periodontopathic bacteria. In this paper, we examine the effects of butyrate on gingival epithelial cells and present evidence that butyrate induces apoptosis and autophagic cell death. In addition, we discuss the possibility that butyrate can break down the epithelial barrier in areas where mature dental plaque with high butyrate concentrations is in contact with gingival epithelial cells.

Material and methods

Materials

Roswell Park Memorial Institute (RPMI) 1640 medium, sodium butyrate and rapamycin were purchased from Wako (Osaka, Japan). Protease inhibitor cocktail, phosphatase inhibitor cocktail and 3-methyladenine, an autophagy inhibitor, were obtained from Sigma-Aldrich (St Louis, MO, USA); anti-microtubule-associated protein 1 light chain 3 (LC3) rabbit polyclonal antibodies and benzyloxycarbonyl-Val-Ala-Asp(O-Me)-fluoromethylketone (Z-VAD-FMK), a caspase family inhibitor, from MBL (Nagoya, Japan); anti-glyceraldehyde-3-phosphate dehydrogenase (GAPDH) mouse monoclonal antibodies and fluorescein isothiocyanate (FITC)-conjugated annexin V from Santa Cruz Biotechnology (Santa Cruz, CA, USA); biotin-conjugated anti-mouse or rabbit immunoglobulin (IgG) from Zymed Laboratories (San Francisco, CA, USA); and [L-3-trans-(propylcarbamoyl)oxirane-2-carbonyl]-L-isoleucyl-L-proline methyl ester (CA-074 Me) from Peptide Institute (Minoh, Japan).

Cell culture

Human gingival epithelial Ca9-22 cells were obtained from the Japanese Collection of Research Bioresources (Health Science Research Resources Bank, Osaka, Japan); these cells have been used previously as culture models of gingival epithelial cells (26–29). The cells were cultured at 37°C in a humidified incubator with 5% CO_2 in RPMI 1640 medium supplemented with heat-inactivated 10% (v/v) fetal bovine serum (FBS) and 1% penicillin–streptomycin (penicillin, 1×10^5 units/L; streptomycin, 100 mg/L; Wako). In order to reduce the possible effects of fatty acid contamination in FBS, 1% FBS was used for sodium butyrate stimulation.

Microscopic observation

The Ca9-22 cells (2×10^5 cells per well) were seeded in 24-well plates, cultured overnight in RPMI 1640 containing

10% FBS, washed with phosphate-buffered saline (PBS, pH 7.5), and incubated at 37°C for 48 h in RPMI 1640 containing 1% FBS in the presence or absence of 10 mM sodium butyrate. Cells were washed with PBS, and FBS-free RPMI 1640 was added to the wells. Microscopic observations were carried out using an IX70 microscope (Olympus, Tokyo, Japan). For the caspase inhibition experiments, 10 μM Z-VAD-FMK was added at the same time as the sodium butyrate.

SYTOX Green cell death assay

The Ca9-22 cells (3.4×10^4 cells per well) were seeded in a black 96-well plate with a transparent bottom (Greiner Bio-One, Frickenhausen, Germany) and cultured overnight in RPMI 1640 containing 10% FBS. The medium in the wells was replaced with 150 μL of phenol red-free RPMI 1640 containing 1% FBS and 0–10 mM sodium butyrate. The plates were incubated for the time indicated. Aliquots of 50 μL of 400 nM SYTOX Green dye (BioVision, Mountain View, CA, USA) in phenol red-free RPMI 1640 were then added, and the plates were incubated in the dark for 15 min. The intensity of fluorescence was measured using a Wallac ArvoSX1420 spectrofluorometer (PerkinElmer, Waltham, MA, USA) with an excitation/emission wavelength of 485/535 nm. For caspase-, autophagy- and cathepsin B-inhibition experiments, the indicated concentrations of a pan-caspase inhibitor (Z-VAD-FMK), an autophagy inhibitor (3-methyladenine) and a cathepsin B inhibitor (CA-074 Me), respectively, were added together with sodium butyrate. The relative cell death was calculated as the percentage of the intensity of fluorescence of each sample against that obtained for the sample untreated with butyrate after subtraction of the background levels. To measure the background fluorescence, equal volumes of phenol red-free RPMI 1640 were added in the staining step instead of RPMI 1640 containing SYTOX Green fluorescent dye. The background value was subtracted from the fluorescence intensity of each sample.

Measurement of early stages of apoptosis using annexin V–FITC

Early apoptotic changes were detected and measured by the identification of externalized phosphatidylserine residues on the cell membrane by using annexin V–FITC. The Ca9-22 cells (3.4×10^4 cells per well) were seeded in a black 96-well plate with a transparent bottom, cultured overnight in RPMI 1640 containing 10% FBS, washed with PBS, and incubated with 100 μL of phenol red-free RPMI 1640 containing 1% FBS in the presence or absence of 10 mM sodium butyrate for the time indicated. Aliquots of 50 μL of phenol red-free RPMI 1640 containing annexin V–FITC were added to the wells, and the plates were incubated in the dark at room temperature for 15 min. After incubation, the plates were centrifuged at 760*g* for 5 min, and 100 μL of the supernatant was removed from each well. The fluorescence intensities were measured using the Wallac ArvoSX1420 spectrophotometer (excitation/emission wavelength, 485/535 nm). To measure the background fluorescence, an equal volume of phenol red-free RPMI 1640 was used in the staining step instead of the RPMI 1640 containing annexin V–FITC. Background fluorescence was subtracted from the fluorescence intensity of each sample.

Caspase-3 activity assay

The Ca9-22 cells (1×10^6 cells per well) were seeded in six-well plates, cultured overnight in RPMI 1640 containing 10% FBS, washed with PBS, and stimulated with or without 10 mM sodium butyrate in RPMI 1640 containing 1% FBS for the time indicated. The cells were then dissociated from the plate using TrypLE Express (Invitrogen, Carlsbad, CA, USA), collected, and stored at −80°C until the assays were performed within 3 d. Cellular caspase-3 activity was determined using the APOPCYTO Caspase-3 Colorimetric Assay kit (MBL) according to the manufacturer's instructions. The results were expressed as relative caspase-3 activity after comparison with the caspase-3 activity of a sample collected at time zero.

Quantitative real-time reverse transcriptase (RT)-PCR

The Ca9-22 cells (1×10^6 cells per well) were seeded in six-well plates, cultured overnight in RPMI 1640 containing 10% FBS, washed with PBS, and incubated in RPMI 1640 containing 1% FBS and 10 mM sodium butyrate for the time indicated. After the dissociation of cells with TrypLE Express, mRNA extraction was performed using a combination of the RNAiso Plus (TaKaRa, Otsu, Japan) and the FastPure RNA Kit (TaKaRa) protocols in order to completely eliminate residual chromosomal DNA. Cloned DNAs were synthesized using PrimeScript RT Reagent Kit (TaKaRa) according to the manufacturer's protocol. The expression of *bcl-2* mRNA, relative to that of the housekeeping gene, β-glucuronidase gene (*gusb*), was measured using a Thermal Cycler Dice Real Time System (TaKaRa) and SYBR Premix Ex Taq (TaKaRa). The primers used in this experiment were obtained from TaKaRa; their sequences are shown in Table 1. After incubation at 95°C for 10 s, 40 PCR cycles were performed with denaturation at 95°C for 5 s, and combined annealing and extension at 60°C for 30 s. To determine the amplification efficiency, standard curves were plotted for each primer set by using the

Table 1. Real-time PCR primers

Primer name	Target	Sequence	NCBI accession number
GUSB-F	*gusb*	5′ -TTTGCGAGTACTCAACACCAACATC -3′	M15182
GUSB-R	*gusb*	5′-CATTATTCAGAGCGAGTATGGAGCA-3′	
BCL2-F	*bcl-2*	5′-GATTGATGGGATCGTTGCCTTA-3′	NM_000633
BCL2-R	*bcl-2*	5′-CCTTGGCATGAGATGCAGGA-3′	

NCBI, National Centre for Biotechnology Information.

threshold cycle (Ct) values obtained from the amplification of serial 10-fold dilutions of cDNA obtained from Ca9-22 cells. Since the amplification efficiencies of *bcl-2* and *gusb* were almost identical (data not shown), a comparative threshold cycle (ΔΔCt) method was used for relative quantification. Data were calculated as the expression levels of mRNA relative to those of the control (0 h) data after normalization with endogenous housekeeping *gusb* expression levels.

Western blotting

The Ca9-22 cells (1×10^6 cells per well) were seeded in six-well plates, cultured overnight in RPMI 1640 containing 10% FBS, washed with PBS, and treated with RPMI 1640 containing 1% FBS and 10 mM sodium butyrate for the indicated time. Ca9-22 cells treated with 100 μM rapamycin for 6 h or RPMI 1640 containing 10% FBS for 2 h were used as the positive or negative controls, respectively. Stimulated cells were dissociated using TrypLE Express, lysed in 1 mL ice-cold lysis buffer (50 mM Tris–HCl, 150 mM NaCl, 1% Triton X-100, phosphatase inhibitor and protease inhibitor cocktail; pH 7.5), and sonicated on ice. After centrifugation at 16,000*g* for 30 min at 4°C, the supernatants from the samples were collected and their total protein concentrations were measured using the Dc Protein Assay kit (Bio-Rad, Hercules, CA, USA). Sodium dodecyl sulfate-polyacrylamide gel electrophoresis (SDS-PAGE) was performed using 5–20% gradient gel and 20 μg protein. Subsequently, the proteins were electrically transferred to Immobilon-P polyvinylidene difluoride membranes (Millipore, Billerica, MA, USA). The membranes were blocked by incubation with Block Ace blocking buffer (Snow Brand Milk Products, Tokyo, Japan) for 1 h. They were then incubated with rabbit anti-LC3 polyclonal antibody or mouse anti-GAPDH monoclonal antibody at dilutions of 1:1000 for 1 h, washed three times in Tris-buffered saline containing 0.1% Tween 20 (TBS-T; pH 7.5), and incubated for 1 h with biotin-conjugated goat anti-rabbit or goat anti-mouse IgG diluted at a ratio of 1:2000 in the blocking buffer. After the membranes had been repeatedly washed with TBS-T, they were treated with streptavidin-peroxidase (KPL, Gaithersburg, MD, USA) for 30 min. Protein bands were visualized by chemiluminescence using an ECL luminescence kit (GE Healthcare, Amersham, UK) and the membranes were exposed to RX-U Medical X-ray Film (Fuji film, Tokyo, Japan). The size of the protein bands was determined using electrophoresis color markers (BioDynamics Laboratory, Tokyo, Japan). The signal intensities of the corresponding bands were measured by a densitometer equipped with ImageJ software (http://rsb.info.nih.gov/ij/). The relative densities were obtained by comparing the band intensities to those of the control (2 h).

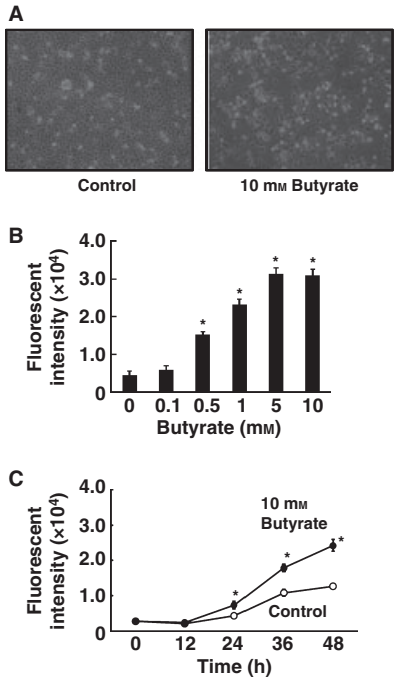

Fig. 1. Induction of gingival epithelial Ca9-22 cell death by butyrate. (A) The Ca9-22 cells were treated with (right panel) or without 10 mM butyrate (left panel) for 48 h and microscopically observed after elimination of floating debris-like cells by washing with PBS. (B) Ca9-22 cells were treated with butyrate at several concentrations for 48 h, and dead cells were stained with SYTOX Green fluorescent dye. The fluorescence emitted was measured using a spectrofluorometer ($n = 4$; $^*p < 0.05$, compared with 0 mM). (C) Time course of death in Ca9-22 cells stimulated with (●) or without 10 mM butyrate (○; $n = 4$; $^*p < 0.05$, compared with the control cells for each time interval).

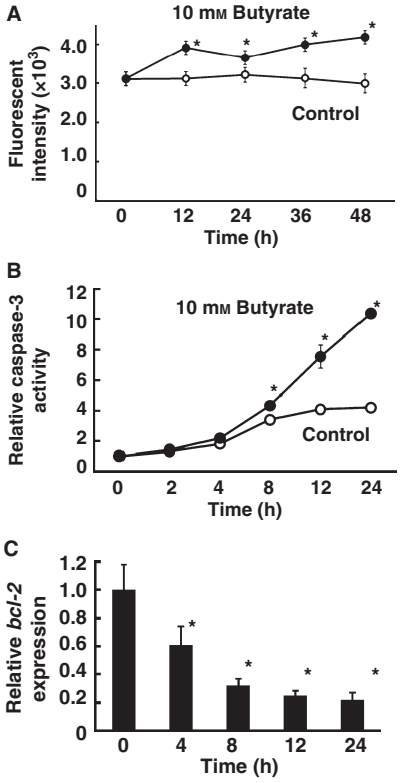

Fig. 2. Butyrate-induced Ca9-22 cell apoptosis. (A) Time course of detected early apoptosis of Ca9-22 cells in the presence (●) or absence of 10 mM butyrate (○). The Ca9-22 cells were treated with or without 10 mM butyrate, and the amount of annexin V–FITC bound to cell surface phosphatidylserine was measured using a spectrofluorometer ($n = 4$; $^*p < 0.05$, compared with the control cells for each time interval). (B) Measurement of caspase-3 activity in Ca9-22 cells after treatment with (●) or without 10 mM butyrate (○) for the time indicated. Relative values for caspase-3 activity were calculated by dividing the values obtained from each sample by those obtained from the sample at time zero ($n = 3$; $^*p < 0.05$, compared with the control cells for each time interval). (C) Time course of the expression of *bcl-2*, an apoptosis suppressor, measured by real-time RT-PCR. The Ca9-22 cells were treated with 10 mM butyrate for the time indicated. Relative values of *bcl-2* mRNA expression levels were calculated with respect to the value calculated for the sample at time zero after normalization with endogenous housekeeping *gusb* expression levels ($n = 3$; $^*p < 0.05$, compared with 0 h).

Fluorescence microscopic analysis of LC3-stained cells

The Ca9-22 cells (2×10^5 cells per well) seeded in 24-well plates were treated with or without 10 mM sodium butyrate for 8 h. Ca9-22 cells treated with 50 μM rapamycin for 6 h or with RPMI 1640 containing 10% FBS for 2 h were used as the positive or negative controls, respectively. Stimulated cells were fixed in 4% formaldehyde for 15 min, washed with PBS three times, and treated with 0.1% Triton X-100 for 15 min. Cells were then incubated for 1 h in PBS containing a 1:1000 dilution of rabbit anti-LC3 polyclonal antibody, washed five times with PBS, and incubated with 10 μg/mL $F(ab')_2$ Fragment-Alexa Fluor 555 (Invitrogen) in PBS for 30 min. After five washes with PBS, the stained cells were observed using the Olympus IX70 fluorescent microscope.

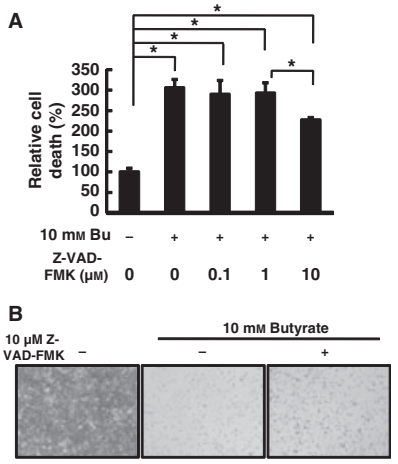

Fig. 3. A pan-caspase inhibitor, Z-VAD-FMK, did not completely inhibit butyrate-induced cell death. (A) The effects of Z-VAD-FMK at varying concentrations on Ca9-22 cell death after stimulation with 10 mM butyrate. Dead cells were stained with SYTOX Green dye, and the death ratios were calculated as the percentage of dead cells relative to that of cells not treated with butyrate ($n = 4$; $*p < 0.05$; Bu, butyrate). (B) Microscopic observations of Ca9-22 cells that were treated for 48 h with 10 mM butyrate in the presence (right panel) or absence of 10 μM Z-VAD-FMK (middle panel) after elimination of floating debris-like cells by PBS washing. Cells not treated with butyrate were used as a control (left panel).

Statistical analysis

Welch's unpaired *t*-test was used for statistical analyses.

Results

Butyrate induced cell death

To investigate the effect of butyrate on gingival epithelial cells, we first treated gingival epithelial Ca9-22 cells with butyrate. As shown in the right panel of Fig. 1A, only a small number of Ca9-22 cells were attached to the plastic plate after 10 mM butyrate treatment for 48 h. Since many floating debris-like structures were seen in the medium (data not shown), the observation was performed after they were eliminated by removal of supernatants and wash with PBS. In contrast, in the absence of butyrate treatment, most of the Ca9-22 cells remained attached to the bottom of the wells (Fig. 1A, left panel).

Cell death was also assessed by using a SYTOX Green cell death assay. The SYTOX Green dye emits a weak fluorescence and does not permeate the cell membranes of live cells. However, on entering a dead cell through a ruptured cell membrane, it intercalates with double-stranded DNA and emits a strong green fluorescence. The resulting fluorescence is therefore proportional to the number of dead cells. Butyrate stimulation for 48 h induced Ca9-22 cell death in a dose-dependent manner, and the effective concentration of butyrate was 0.5 mM or more (Fig. 1B). Similar levels of fluorescence were emitted after 5 and 10 mM butyrate treatment (Fig. 1B). The time course for the effect of butyrate exposure on Ca9-22 cell death was also measured. The proportion of dead Ca9-22 cells was significantly greater in the presence of 10 mM butyrate than in the butyrate-untreated control cultures at and after 24 h (Fig. 1C). Interestingly, a certain number of Ca9-22 cells also died in the absence of butyrate at 36 h or later (Fig. 1C).

Butyrate induced apoptosis

To investigate the observed phenomenon, we hypothesized that it may be due to apoptosis. We first measured an annexin V binding to the cell surface, one of the markers in the early stage of apoptosis, which redistributes phosphatidylserine from the cytoplasmic interface to the extracellular surface of the cell membrane. Ca9-22 cells treated with 10 mM butyrate exhibited weak annexin V–FITC-derived fluorescence, but stronger than that of the butyrate-untreated control cultures at and after 12 h (Fig. 2A).

In order to confirm apoptosis, we then measured caspase-3 activity and *bcl-2* mRNA expression of Ca9-22 cells in the presence of 10 mM butyrate. Caspase-3 activation and *bcl-2* down-regulation are one of the most impor-

Fig. 4. Inhibition of butyrate-induced autophagy suppressed butyrate-induced cell death. (A) The Ca9-22 cells were treated either with or without 10 mM butyrate for 48 h in the presence of the indicated concentrations of 3-methyladenine, an autophagy inhibitor. Dead cells were stained with SYTOX Green fluorescent dye, and the fluorescence emitted was measured using a spectrofluorometer. The relative cell death was calculated as the percentage of dead cells relative to that of cells not treated with butyrate or 3-methyladenine ($n = 4$; $*p < 0.05$; Bu, butyrate; 3MA, 3-methyladenine). (B) The Ca9-22 cells were treated with or without 10 mM butyrate for the time indicated, and cell lysates were analyzed by western blotting. The LC3-I and LC3-II bands were detected using rabbit anti-LC3 polyclonal antibodies. Levels of GAPDH were also detected as an internal control. The densities of each band were measured by densitometry, and the relative band densities were calculated by comparing the band densities with those of the control (2 h). Abbreviations: Bu, 10 mM butyrate treatment; Fed, 10% FBS treatment for 2 h; and Rapa, 100 μM rapamycin treatment for 6 h. (C) The Ca9-22 cells were cultured in the presence (Ca) or absence of 10 mM butyrate (Cb) for 8 h. Immunocytochemistry was performed with rabbit anti-LC3 polyclonal antibodies and Alexa Fluor 555-conjugated goat anti-rabbit $F(ab')_2$ fragments. The arrowheads indicate LC3-II accumulation. The experiment for background data was performed without rabbit anti-LC3 polyclonal antibodies (Cc). Also shown are Ca9-22 cells treated with 10% FBS for 2 h (Fed; Cd) and Ca9-22 cells treated for 6 h with 50 μM rapamycin (Rapa; Ce).

tant events during apoptosis signaling. The caspase-3 activity of Ca9-22 cells treated with 10 mM butyrate for more than 8 h was significantly higher than that of the untreated control cells (Fig. 2B). In addition, the mRNA expression of *bcl-2* was significantly decreased by 10 mM butyrate after 4 h (Fig. 2C). These results suggest that high concentrations of butyrate induce apoptosis.

Z-VAD-FMK, a pan-caspase inhibitor, did not completely inhibit butyrate-induced cell death

In order to further investigate butyrate-induced apoptosis, we inhibited the caspase activity of Ca9-22 cells using a cell membrane-permeable pan-caspase inhibitor, Z-VAD-FMK, during butyrate stimulation. In a preliminary experiment, 10 μM Z-VAD-FMK inhibited butyrate-induced caspase-3 activity completely (Fig. S1). Treatment with 10 μM of Z-VAD-FMK inhibited 10 mM butyrate-induced cell death to some extent but not completely (Fig. 3A). This was also observed microscopically (Fig. 3B). Commercially obtained Z-VAD-FMK was dissolved in dimethylsulfoxide (DMSO) such that the concentration of DMSO in the media containing 10 μM Z-VAD-FMK was 0.1%. Thus, we also examined the effect of 0.1% DMSO on butyrate-induced cell death by using the SYTOX Green cell death assay. The cell death induced by 10 mM butyrate was not affected by the 0.1% DMSO in the media (Fig. S2).

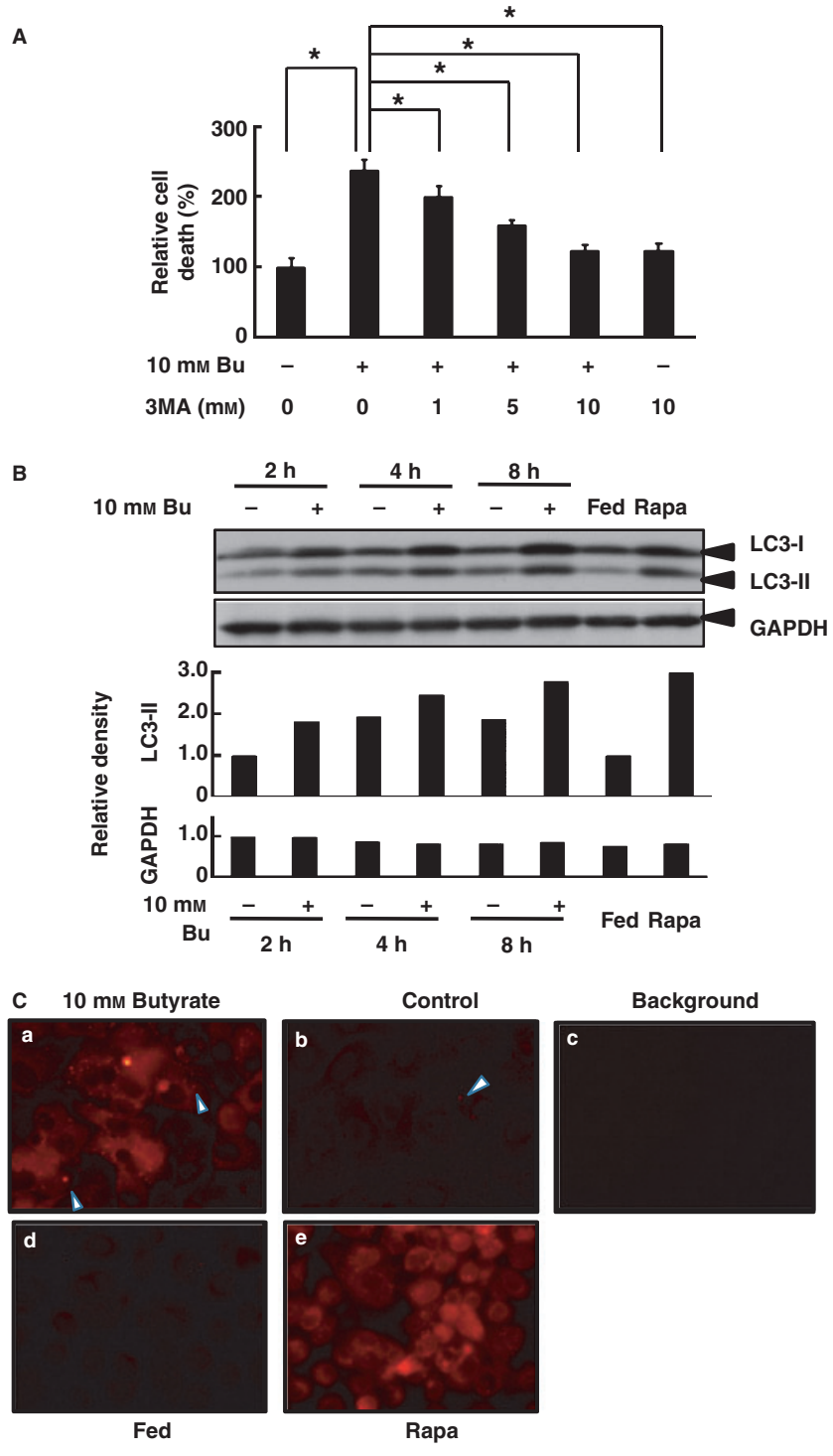

Butyrate induced autophagic cell death

Since the caspase inhibitor did not completely suppress butyrate-induced Ca9-22 cell death, we examined the involvement of autophagic cell death, another important physiological cell death process, using a autophagy inhibitor, 3-methyladenine. Treatment of Ca9-22 cells with 3-methyladenine significantly suppressed cell death induced by 10 mM butyrate in a dose-dependent manner (Fig. 4A).

In order to obtain further confirmation that cell death induced by butyrate was autophagic cell death, we next examined the effect of CA-074 Me, a cathepsin B inhibitor. During autophagic cell death, excess amounts of important cytoplasmic components engulfed by autophagosomal membranes are digested by lysosomal enzymes such as cathepsin B, and this phenomenon is indispensable to autophagic cell death (30). Treatment of Ca9-22 cells with CA-074 Me significantly suppressed the cell death induced by 10 mM butyrate in a dose-dependent manner (Fig. S3).

During autophagy, a cytosolic form of LC3-I is converted into an autophagosome-associated form (LC3-II)

by covalent conjugation of a phosphatidylethanolamine to LC3-I. Then, LC3-II is recruited to autophagosomal membranes. Owing to the highly hydrophobic nature of phosphatidylethanolamine, LC3-II is more hydrophobic than LC3-I. Therefore, LC3-II appears to be smaller than LC3-I on western blot. The Ca9-22 cells treated with rapamycin, which is a strong inducer of autophagy, showed a more prominent LC3-II band than 10% FBS-treated fed cells (Fig. 4B). To obtain additional confirmation of butyrate-induced autophagic cell death, we examined the conversion of LC3-I to LC3-II using western blot. The LC3-I and LC3-II bands were more prominent for butyrate-treated cells than for control cells, while the intensities of the internal control (GAPDH) bands were not affected by butyrate stimulation (Fig. 4B).

In addition, LC3-II accumulation was observed by fluorescence microscopic analysis using anti-LC3 antibody. Cells treated with rapamycin, an autophagy inducer (Fig. 4Ce) showed stronger red fluorescence derived from LC3 accumulation in their cytosol than fed cells (Fig. 4Cd). In the same fashion, stronger fluorescence spots (indicated by arrowheads) were observed in Ca9-22 cells that were treated with 10 mM butyrate than control cells (Fig. 4Ca, 4Cb).

Discussion

In this study, we demonstrated that butyrate induced death of gingival epithelial cells. This effect was largely inhibited by an autophagy inhibitor and cathepsin B inhibitor, suggesting that the cell death was induced by autophagy (Figs 1,4A,S3). In addition, pan-caspase inhibition partly suppressed cell death (Fig. 3). These observations suggest the occurrence of butyrate-induced caspase-independent autophagic cell death. Some apoptotic markers were also detected in these cells (Fig. 2). Therefore, we conclude that butyrate induces the death of gingival epithelial Ca9-22 cells primarily via caspase-independent autophagy and partly via apoptosis.

Although apoptosis and autophagic cell death are classified separately (15,24), these two types of cell death are thought to have extremely complex interrelationships. It has been reported that autophagy frequently occurs with apoptosis and that numerous stimuli can induce either apoptosis, autophagy, or both (21). Some upstream signaling molecules are common to both processes (22–24), and the interaction between them may arise as a result of signaling cross-talk. However, the exact mechanism of these interactions still remains unclear. Our results indicated that butyrate induced both apoptosis and autophagic cell death in gingival epithelial cells, while a previous study has demonstrated that butyrate induces apoptosis in T-cell lymphocytes (31). The butyrate-induced T-cell apoptosis is reportedly mediated by ceramide production, reactive oxygen species synthesis in mitochondria, and subsequent JNK (c-Jun N-terminal kinase) activation in the MAPK cascade (31). In contrast, the exact mechanism underlying butyrate-induced gingival epithelial cell death is still unknown. These phenotypic differences may also arise from the complex relationship between apoptosis and autophagy.

Autophagy is a process of regulated degradation and recycling of cytoplasmic components for organelle turnover and the management of energy during nutrient starvation. However, excessive autophagy leads to cell death (19,21). In our study, we observed that Ca9-22 cell death was induced not only in the presence but also in the absence of butyrate after incubation for 24 h or more (Fig. 1C). The cell death induced in the absence of butyrate may be due to the occurrence of excessive autophagy caused by long-term ($>$ 24 h) nutrient shortage. In fact, we observed traces of LC3 accumulation in cells, one of the markers of autophagy, even in control cells (Fig. 4Cb). Moreover, the effect of butyrate on Ca9-22 cells in fed conditions (media containing 10% FBS) was weaker than that in starved conditions (data not shown). Therefore, starved conditions may play a role in induction of death in butyrate-treated Ca9-22 cells. In mature dental plaque, periodontopathic bacteria produce butyrate. In addition, gingival epithelial cells in the periodontal crevices may face severe nutrient shortage because they compete with a large number of bacteria in the mature dental plaque for nutrients from the crevicular fluid. In such conditions, the death of gingival epithelial cells in the periodontal crevices, particularly of those in contact with the mature dental plaque, may be easily induced by butyrate and starvation.

The concentrations of butyrate in the subgingival plaque and the gingival crevicular fluid of patients with periodontal diseases have been reported to be 2.6–14 and 0.33–1.14 mM, respectively (9,10,13). Therefore, the gingival epithelial cells surrounding the gingival crevices may be susceptible to millimolar concentrations of butyrate, and the cells in contact with mature dental plaque, in particular, may be susceptible to butyrate concentrations that exceed 10 mM. Since our results indicate that treatment with 0.5–10 mM butyrate could induce gingival epithelial cell death, we propose that the butyrate produced in mature subgingival plaque and gingival crevicular fluid can potentially result in gingival epithelial cell death. Butyrate may thus play an important role in killing gingival epithelial cells and subsequent breakdown of the integrity of the front-line epithelial barrier of gingival tissues. Moreover, butyrate has been reported to induce apoptosis in T- and B-lymphocytes (5,32) and to stimulate the release of proinflammatory cytokines by neutrophils (8). Once the epithelial integrity is compromised by the action of butyrate produced by periodontal pathogens, butyrate may penetrate into the underlying, highly vascularized connective tissue and consequently induce apoptosis of T- and B-lymphocytes and cytokine release by neutrophils. This may mean that butyrate is one of the initiators and inducers of periodontal disease. Therefore, it might be efficacious to eliminate or inhibit the effects of butyrate to prevent periodontal diseases.

To summarize, our results suggest that butyrate induces not only apoptosis but also autophagic cell death in

gingival epithelial Ca9-22 cells and that autophagic cell death occurs in a caspase-independent manner. In addition, we propose a potential role of butyrate, a bacterial metabolite, in the pathogenesis of periodontal disease. Further investigations to elucidate the mechanisms of butyrate-induced autophagic cell death and butyrate production by bacteria may be useful in developing methods for the prevention of periodontal disease.

Acknowledgements

This work was supported by a Grant-in-Aid for Young Scientists (HT, B19791641) from the Ministry of Education, Culture, Sports, Science and Technology of Japan, a Nihon University Joint Research Grant (KO, NS, HT, 2008), a Nihon University Individual Research Grant for Assistants and Young Researchers (HT, 2008), an Uemura fund, Nihon University School of Dentistry, and a Grant from Dental Research Center, Nihon University School of Dentistry (HT, 2008).

Supporting information

Additional Supporting Information may be found in the online version of this article:

Figure S1. Ten micromolar of Z-VAD-FMK completely inhibited butyrate-induced caspase-3 activity. Ca9-22 cells were treated with 10 mM butyrate for 16 h in the presence or absence of 10 μM Z-VAD-FMK and the caspase-3 activities were measured. Cells that were not treated with butyrate were used as the control. The caspase-3 activities relative to the control are indicated ($n = 3$; $*p < 0.05$; Bu, butyrate).

Figure S2. DMSO (0.1%), a diluent of Z-VAD-FMK, did not cause butyrate-induced Ca9-22 cell death. Ca9-22 cells were treated with 10 mM butyrate for 48 h in the presence or absence of 0.1% DMSO, which corresponded to the concentration of DMSO contained in 10 μM Z-VAD-FMK. Dead cells were stained with the SYTOX Green fluorescent dye, and the fluorescence emitted was measured by using a spectrofluorometer. The relative cell death was calculated as the percentage of dead cells to that of control ($n = 4$; $*p < 0.05$; Bu, butyrate).

Figure S3. Cathepsin B inhibitor, CA-074Me, decreased butyrate-induced Ca9-22 cell death. Ca9-22 cells were treated either with or without 10 mM butyrate for 48 h in the presence of the indicated concentrations of CA-074 Me. Dead cells were stained with SYTOX Green fluorescent dye, and the fluorescence emitted was measured using a spectrofluorometer. The relative cell death was calculated as the percentage of dead cells to that of cells not treated with butyrate or CA-074 Me ($n = 4$; $*p < 0.05$; Bu, butyrate).

Please note: Wiley-Blackwell are not responsible for the content or functionality of any supporting materials supplied by the authors. Any queries (other than missing material) should be directed to the corresponding author for the article.

References

1. Singer RE, Buckner BA. Butyrate and propionate: important components of toxic dental plaque extracts. *Infect Immun* 1981;**32:**458–463.
2. Jeng JH, Chan CP, Ho YS, Lan WH, Hsieh CC, Chang MC. Effects of butyrate and propionate on the adhesion, growth, cell cycle kinetics, and protein synthesis of cultured human gingival fibroblasts. *J Periodontol* 1999;**70:**1435–1442.
3. Gamet L, Daviaud D, Denis-Pouxviel C, Remesy C, Murat JC. Effects of short-chain fatty acids on growth and differentiation of the human colon-cancer cell line HT29. *Int J Cancer* 1992;**52:**286–289.
4. Eftimiadi C, Tonetti M, Cavallero A, Sacco O, Rossi GA. Short-chain fatty acids produced by anaerobic bacteria inhibit phagocytosis by human lung phagocytes. *J Infect Dis* 1990;**161:**138–142.
5. Kurita-Ochiai T, Fukushima K, Ochiai K. Butyric acid-induced apoptosis of murine thymocytes, splenic T cells, and human Jurkat T cells. *Infect Immun* 1997;**65:**35–41.
6. Schroeder TM, Westendorf JJ. Histone deacetylase inhibitors promote osteoblast maturation. *J Bone Miner Res* 2005;**20:**2254–2263.
7. Katono T, Kawato T, Tanabe N *et al.* Sodium butyrate stimulates mineralized nodule formation and osteoprotegerin expression by human osteoblasts. *Arch Oral Biol* 2008;**53:**903–909.
8. Niederman R, Zhang J, Kashket S. Short-chain carboxylic-acid-stimulated, PMN-mediated gingival inflammation. *Crit Rev Oral Biol Med* 1997;**8:**269–290.
9. Pollanen MT, Salonen JI, Uitto VJ. Structure and function of the tooth-epithelial interface in health and disease. *Periodontol 2000* 2003;**31:**12–31.
10. Botta GA, Radin L, Costa A, Schito G, Blasi G. Gas-liquid chromatography of the gingival fluid as an aid in periodontal diagnosis. *J Periodontal Res* 1985;**20:**450–457.
11. Tonetti M, Eftimiadi C, Damiani G, Buffa P, Buffa D, Botta GA. Short chain fatty acids present in periodontal pockets may play a role in human periodontal diseases. *J Periodontal Res* 1987;**22:**190–191.
12. Kurita-Ochiai T, Fukushima K, Ochiai K. Volatile fatty acids, metabolic by-products of periodontopathic bacteria, inhibit lymphocyte proliferation and cytokine production. *J Dent Res* 1995;**74:**1367–1373.
13. Niederman R, Buyle-Bodin Y, Lu BY, Robinson P, Naleway C. Short-chain carboxylic acid concentration in human gingival crevicular fluid. *J Dent Res* 1997;**76:**575–579.
14. Pollanen MT, Salonen JI. Effect of short chain fatty acids on human gingival epithelial cell keratins in vitro. *Eur J Oral Sci* 2000;**108:**523–529.
15. Lockshin RA, Zakeri Z. Apoptosis, autophagy, and more. *Int J Biochem Cell Biol* 2004;**36:**2405–2419.
16. Wyllie AH. Glucocorticoid-induced thymocyte apoptosis is associated with endogenous endonuclease activation. *Nature* 1980;**284:**555–556.
17. Wyllie AH, Kerr JF, Currie AR. Cell death: the significance of apoptosis. *Int Rev Cytol* 1980;**68:**251–306.
18. Earnshaw WC. Nuclear changes in apoptosis. *Curr Opin Cell Biol* 1995;**7:**337–343.
19. Cuervo AM. Autophagy: in sickness and in health. *Trends Cell Biol* 2004;**14:**70–77.
20. Gonzalez-Polo RA, Boya P, Pauleau AL *et al.* The apoptosis/autophagy paradox: autophagic vacuolization before apoptotic death. *J Cell Sci* 2005;**118:**3091–3102.
21. Levine B, Yuan J. Autophagy in cell death: an innocent convict? *J Clin Invest* 2005;**115:**2679–2688.
22. Pattingre S, Tassa A, Qu X *et al.* Bcl-2 antiapoptotic proteins inhibit Beclin 1-dependent autophagy. *Cell* 2005;**122:**927–939.
23. Maiuri MC, Zalckvar E, Kimchi A, Kroemer G. Self-eating and self-killing: crosstalk between autophagy and apoptosis. *Nat Rev Mol Cell Biol* 2007;**8:**741–752.
24. Nishida K, Yamaguchi O, Otsu K. Crosstalk between autophagy and apop-

tosis in heart disease. *Circ Res* 2008;**103:** 343–351.
25. Shimizu S, Kanaseki T, Mizushima N *et al*. Role of Bcl-2 family proteins in a non-apoptotic programmed cell death dependent on autophagy genes. *Nat Cell Biol* 2004;**6:**1221–1228.
26. Hirose K, Isogai E, Mizugai H, Ueda I. Adhesion of Porphyromonas gingivalis fimbriae to human gingival cell line Ca9-22. *Oral Microbiol Immunol* 1996;**11:** 402–406.
27. Ohshima M, Noguchi Y, Ito M, Maeno M, Otsuka K. Hepatocyte growth factor secreted by periodontal ligament and gingival fibroblasts is a major chemoattractant for gingival epithelial cells. *J Periodontal Res* 2001;**36:**377–383.
28. Takeuchi H, Setoguchi T, Machigashira M, Kanbara K, Izumi Y. Hydrogen sulfide inhibits cell proliferation and induces cell cycle arrest via an elevated p21 Cip1 level in Ca9-22 cells. *J Periodontal Res* 2008;**43:**90–95.
29. Saito A, Inagaki S, Kimizuka R *et al*. Fusobacterium nucleatum enhances invasion of human gingival epithelial and aortic endothelial cells by Porphyromonas gingivalis. *FEMS Immunol Med Microbiol* 2008;**54:**349–355.
30. Uchiyama Y. Autophagic cell death and its execution by lysosomal cathepsins. *Arch Histol Cytol* 2001;**64:**233–246.
31. Kurita-Ochiai T, Amano S, Fukushima K, Ochiai K. Cellular events involved in butyric acid-induced T cell apoptosis. *J Immunol* 2003;**171:**3576–3584.
32. Kurita-Ochiai T, Ochiai K, Fukushima K. Volatile fatty acid, metabolic by-product of periodontopathic bacteria, induces apoptosis in WEHI 231 and RAJI B lymphoma cells and splenic B cells. *Infect Immun* 1998;**66:**2587–2594.